Extremely small diffusion constant of Cs in multiwalled carbon nanotubes

S. Suzuki,[a] Y. Watanabe, and T. Ogino
NTT Basic Research Laboratories, Atsugi, Kanagawa 243-0198, Japan

S. Heun, L. Gregoratti, A. Barinov, B. Kaulich, and M. Kiskinova
Sincrotrone Trieste, Basovizza, 34012 Trieste, Italy

W. Zhu
Bell Laboratories, Lucent Technologies, Murray Hill, New Jersey 07974

C. Bower[b] and O. Zhou
Department of Physics and Astronomy and Curriculum in Applied and Materials Sciences, University of North Carolina at Chapel Hill, Chapel Hill, North Carolina 27599

(Received 29 July 2002; accepted 9 October 2002)

The Cs intercalation process in multiwalled carbon nanotubes (MWNTs) was studied by cross-sectional scanning photoemission microscopy. Cs atoms initially deposited on the tips of aligned nanotubes diffused toward their roots. The Cs diffusion constant for the MWNTs at room temperature was evaluated from the Cs distribution measured along the axes of the tubes. The value of 2×10^{-12} cm^2/s obtained is seven orders of magnitude smaller than that in graphite, although the local atomic structure of an intercalated MWNT is very similar to that of intercalated graphite. [DOI: 10.1063/1.1525401]

I. INTRODUCTION

Syntheses of nanotube intercalation compounds and their electronic properties have been extensively investigated, because the physical and chemical properties of carbon nanotubes can be widely controlled by intercalation predominantly due to charge transfer between the nanotube and the guest species.[1–4] Intercalation into nanotubes has also been studied in terms of the development of high energy density lithium rechargeable batteries.[5,6] For multiwalled nanotubes (MWNTs), guest species are inserted between adjacent graphene sheets, as well as in graphite intercalation compounds.[7] For single walled nanotube (SWNT) bundles, intercalants are inserted between the SWNTs.[8,9] They can also be inserted into the interior space of individual open-ended SWNTs.[5,10] Up to now, various elements and molecules, such as alkali metals,[1–4] halogens,[1,2,11] and fullerenes,[10] have been found to form intercalation compounds with nanotubes. However, very little is known about diffusion dynamics in nanotubes, mainly because of experimental difficulties that arise due to their size.

We used photoelectron spectromicroscopy to investigate directly the diffusion of Cs in MWNTs by probing the lateral distribution of Cs along the axes of the nanotubes following Cs deposition on the tips of aligned MWNTs. These studies follow our previous spectromicroscopy analysis of a highly aligned MWNT sample, and have revealed a strong position dependence of the density of states near the Fermi level.[12] The scanning photoemission microscopy (SPEM) utilized allows mapping of the elemental lateral distribution and detailed spectroscopic analysis of the composition in the microspot using as fingerprints the photoelectrons emitted from selected core or valence levels.[13,14] In the present study, the Cs distribution a certain time after Cs deposition was directly visualized by Cs $4d$ photoelectron microscopy images and was used to elucidate the Cs diffusion constant in MWNTs. The diffusion constant obtained in MWNTs was found to be much smaller than that in graphite.

II. EXPERIMENT AND METHODOLOGY

MWNTs aligned perpendicularly on a Si substrate were grown using microwave plasma-enhanced chemical vapor deposition (MPE-CVD) with Co as a catalyst. A typical cross-sectional scanning electron microscope (SEM) image of a cleaved sample is shown in Ref. 12. The diameter and length of the nanotubes were about 30 nm and 10 μm, respectively. The catalytic Co particles are encapsulated at the bottom of the nanotubes.[15] The synthesis and structural properties of these MWNT samples are described in detail elsewhere.[15,16]

Photoelectron spectromicroscopy experiments were performed with the SPEM station attached to the ESCA microscopy beamline at the ELETTRA synchrotron radiation light source in Trieste, Italy. The microscope consists of a photon focusing system (a combination of a Fresnel zone plate lens and an order sorting aperture), a specimen positioning and scanning system, and a hemispherical capacitor electron analyzer with a 16-channel detector. The angle between the incident light (normal to the sample) and the electron energy analyzer is 70°. The instrument works in imaging and spectroscopy modes. Detailed descriptions of the beamline and measurement station are given elsewhere.[13,14] All cross-sectional spectromicroscopy measurements reported here were carried out with lateral resolution of 90 nm and energy resolution of about 0.3 eV (photon energy: 497.0 eV). Under

[a]Electronic mail: ssuzuki@will.brl.ntt.co.jp
[b]Present address: Inplane Photonics, South Plainfield, NJ 07080.

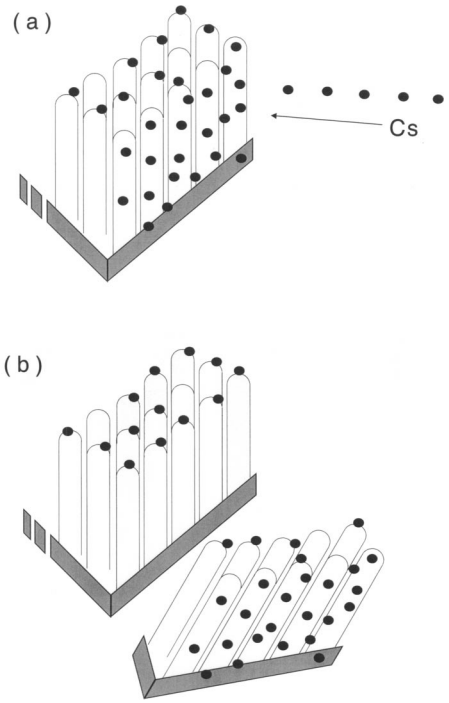

FIG. 1. Schematics of our sample preparation for observing the Cs intercalation process.

these conditions, the probing depth of our experiments is a few nanometers (of the order of 10 graphene layers).

The MWNT sample was annealed at about 200 °C for 12 h in the preparation chamber (base pressure $\sim 5 \times 10^{-10}$ Torr) in order to remove physisorbed molecules.[17] As we have already demonstrated using conventional photoemission spectroscopy, Cs intercalation into MPE-CVD grown aligned MWNTs can be achieved by Cs deposition on the sample in vacuum using a Cs dispenser.[17] Direct observation of Cs intercalation was also reported in our previous transmission electron microscopy (TEM) study of MWNTs synthesized by the arc-discharge method.[7] In the present study, we used the following procedure in order to observe the Cs intercalation process. Cs was deposited at a grazing angle about 80° to the surface of the aligned MWNT sample in the preparation chamber at about 293 and 373K. As illustrated in Fig. 1(a), this procedure results in Cs deposition only on the tips (the surface of the sample) and on the sidewalls of MWNTs at the side of the sample facing the evaporator. In order to remove MWNTs on this side, the sample was cleaved [see Fig. 1(b)]. After cleavage, only the tips of the MWNTs remain covered with Cs, so we can monitor how these Cs atoms diffuse from the tips toward the roots by intercalation. The measurements of Cs distribution along the tube axes were carried out in the SPEM analysis chamber (base pressure: $\sim 1 \times 10^{-10}$ Torr), to which the sample was transferred after cleavage.

Since SPEM images of the sample were rather strongly affected by the topography, we needed to apply some processing procedure in order to better visualize the Cs distribution. Figure 2(a) shows a cross-sectional C 1*s* SPEM image of the aligned MWNT sample obtained by collecting photoelectrons within a 4.4 eV energy range including the C

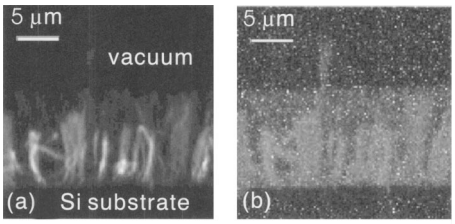

FIG. 2. Cross-sectional C 1*s* SPEM images of aligned MWNTs (a) before and (b) after data processing. The dimension of the images is 25.6 $\times 25.6\ \mu m^2$.

1*s* emission peak (binding energy: about 284.5 eV). The contrast in this image is dominated by the surface topography, which is enhanced by the grazing acceptance angle of the analyzer. That is why the MWNT bundles facing the analyzer appear very bright, whereas other parts are very dark due to a shadowing effect by neighboring nanotubes. The topographic effects, which obscure the Cs concentration distribution, can be significantly reduced using well established image processing procedures.[18,19] The procedure we used can be described by the relationship $(I_{\text{int}} - I_{bg})/I_{bg}$, where, I_{int} is the image of the total photoelectron signal within the energy window collected by the 16-channel detector, which is the sum of the C 1*s* core-level emission and the background secondary electron signal, and I_{bg} is the image obtained by collecting the secondary electron emission in the vicinity of the C 1*s* line. The resulting image with a strongly reduced topographic artifact is shown in Fig. 2(b). By dividing the two images, we also remove the effect of changes in the photon flux intensity, so that the processed maps can be used for quantitative evaluations.

III. DATA ANALYSIS

We evaluated the Cs diffusion constant in the MWNTs from the Cs distribution along the tube axes a certain time after Cs deposition. Here, we explicitly consider Cs diffusion only in the direction along the tube axes. In the one-dimensional approximation, the Cs concentration $c(x,t)$ in a nanotube $(0 \leqslant x \leqslant l)$ is given by the following diffusion equation:

$$\frac{\partial c}{\partial t} = D(T)\frac{\partial^2 c}{\partial x^2}, \tag{1}$$

where $D(T)$ is the diffusion constant at temperature T, x is the coordinate along the tube axis, and t is the time after Cs deposition. For simplicity, we assume that at $t=0$ Cs atoms whose total number is c_0 are located at the tip of the nanotube $(x=0)$ in δ-functional form. That is, the initial condition is given by

$$c(x,0) = c_0\delta(+0). \tag{2}$$

We also assume that the Cs atoms diffuse only within the length of the nanotube and cannot desorb or penetrate into the Si substrate. Thus, the boundary conditions can be written as

$$\left.\frac{\partial c}{\partial x}\right|_{x=0} = 0, \quad \left.\frac{\partial c}{\partial x}\right|_{x=l} = 0. \tag{3}$$

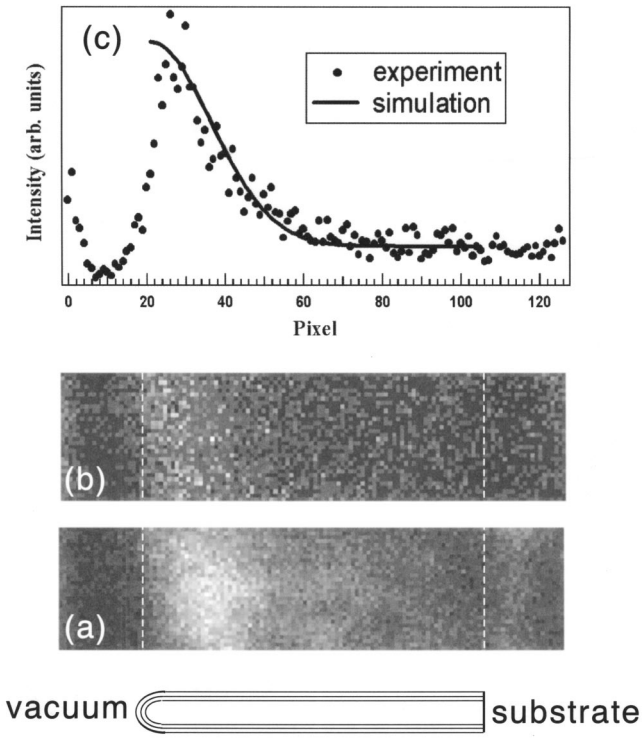

FIG. 3. Results of Cs diffusion in aligned MWNTs at 293 K. The data are obtained 72 min after Cs deposition. (a) Cross-sectional Cs 4*d* SPEM image before data processing. (b) Cross-sectional Cs 4*d* image after data processing. The dimension of both the images (a) and (b) is $2.56\times10.24\ \mu m^2$. (c) Cs distribution along the tube axes obtained from (b).

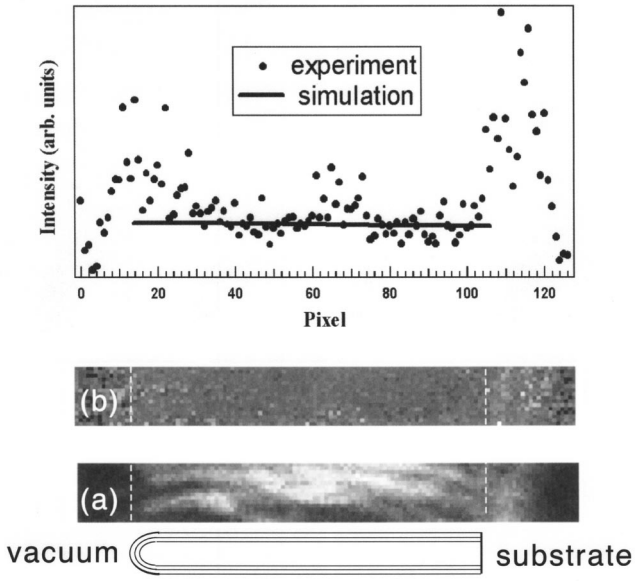

FIG. 4. Results of Cs diffusion at 373 K. The data are obtained 108 min after Cs deposition. (a) Cross -sectional Cs 4*d* SPEM image before data processing. (b) Cross-sectional Cs4*d* image after data processing. The dimension of both the images (a) and (b) is $1.92\times15.36\ \mu m^2$. (c) Cs distribution along the tube axes obtained from (b).

There should be a saturation Cs/C ratio for Cs-intercalated MWNTs (CsC_8 for graphite). However, in this calculation, we ignore it because, as shown below, the observed Cs distribution after Cs diffusion did not saturate even near the tips.

From symmetry, this problem is mathematically equivalent to that of diffusion within a length of $2l$ ($-l\leqslant x\leqslant l$), if the initial Cs distribution is replaced by $c(x,0)$ ($-l\leqslant x\leqslant l$), which satisfies $c(-x)=c(x)$. Thus, the initial condition can be replaced by

$$c(x,0)=2c_0\delta(0). \tag{4}$$

The boundary conditions, Eqs. (3), can also be replaced by

$$\left.\frac{\partial c}{\partial x}\right|_{x=-l}=0, \quad \left.\frac{\partial c}{\partial x}\right|_{x=l}=0. \tag{5}$$

Now, we can avoid the mathematical difficulty caused by the δ function at the system boundary. Diffusion equation (1) can be solved under initial and boundary conditions, Eqs. (4) and (5), and we obtain

$$c(x,t)=\frac{1}{l}+\frac{2}{l}\sum_{r=1}^{\infty}\exp\left(-\frac{(r\pi)^2D}{l^2}t\right)\cos\left(\frac{r\pi x}{l}\right). \tag{6}$$

Thus, the Cs diffusion constant D was evaluated by fitting the experimentally obtained Cs concentration profile.

IV. RESULTS AND DISCUSSION

Figure 3 shows original and topography corrected Cs 4*d* SPEM images of the sample 72 min after Cs deposition at 293 K. Unfortunately, we could not obtain this image sooner, because, after Cs deposition, the cleavage, sample transfer into the SPEM system, and fine focusing usually require more than 1 h. The Cs concentration profile shown in Fig. 3(c) was obtained by integrating the normalized Cs 4*d* intensity in Fig. 3(b) along the vertical direction. This procedure further reduces the topographic effects and improves the statistics. The lateral Cs distribution clearly shows that Cs atoms, initially deposited on the tips, have diffused about 3.5 μm from the tips. There are two possible routes for Cs diffusion. One is through the adjacent graphene sheets by intercalation, and the other is on the surface of nanotube walls. As discussed below, however, the Cs distribution occurs via an intercalation process in this case. A curve fitting result obtained by a solution of the one-dimensional diffusion equation, Eq. (6), is also shown in Fig. 3(c). The diffusion constant $D_{293\,K}$ was evaluated to be 2×10^{-12} cm^2/s.

As one would expect, a large temperature dependence was observed in the Cs diffusion. Figure 4 shows results obtained 108 min after Cs deposition at 373 K. In this case, Cs atoms had diffused more quickly and reached the substrate. The measured concentration profile shows that the Cs atoms have segregated at the tips and the roots of the nanotubes, whereas along the tube axes they are almost uniformly distributed, indicating that the system has almost reached equilibrium. From the curve fitting results shown in Fig. 4(c), the Cs diffusion constant $D_{373\,K}$ is evaluated to be at least larger than 8×10^{-11} cm^2/s. By combining the results at 293 and at 373 K and assuming activation type temperature dependence of $D[=D_0\exp(-E_a/kT)]$, we evaluate the activation energy E_a to be less than 0.45 eV.

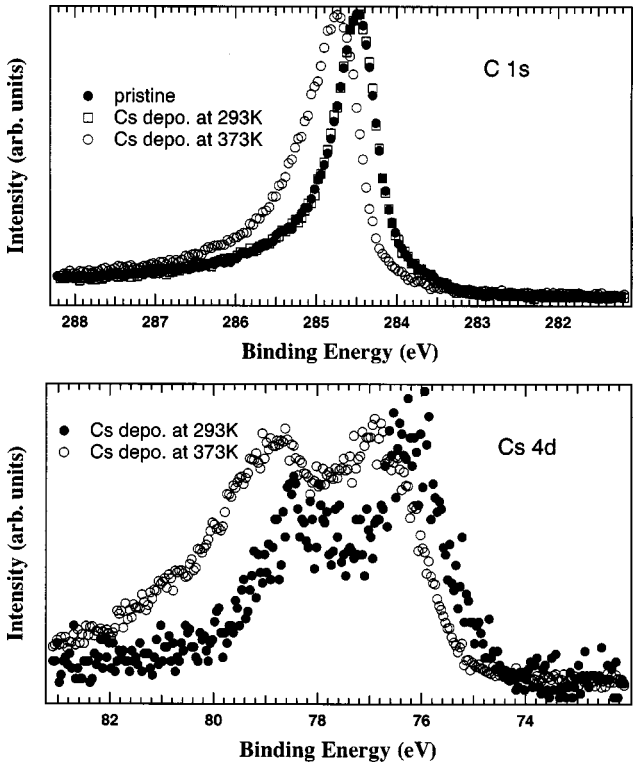

FIG. 5. C 1*s* and Cs 4*d* spectra from sidewalls of Cs-deposited MWNTs. Cs was deposited on the MWNT tips at 293 and 373 K. The C 1*s* spectrum from the sidewalls of pristine MWNTs is also shown for comparison.

Figure 5 shows C 1*s* and Cs 4*d* spectra obtained from sidewalls of MWNTs after Cs deposition at 293 and 373 K. The spectra were obtained about 270 (293 K) and 210 (373 K) min after Cs deposition. Cs was also observed from the sidewalls due to diffusion. The Cs 4*d*/C 1*s* photoelectron intensity ratios of the sidewalls of the MWNTs deposited at 293 and 373 K were 0.13 and 0.08, respectively. The Cs/C atomic ratios were estimated to be of order of a few percent. For the sake of comparison, the C 1*s* spectrum from the sidewalls of pristine MWNTs is shown as well in the C 1*s* panel. Before the Cs depositions, we did not observe any position dependence of the C 1*s* spectra within the sidewalls, as reported in a previous study.[12]

As can be seen in Fig. 5, both the C 1*s* and Cs 4*d* spectra of MWNTs with Cs deposited at 373 K are broadened at the higher binding energy side. The peak positions are also shifted toward the higher binding energy sides by about 0.3 eV. A similar tail structure and binding energy shift have been observed for many years by x-ray photoelectron spectroscopy studies of alkali-metal-intercalated graphite, and ascribed to intrinsic broadening caused by the intercalation.[20,21] However, on the other hand, the MWNTs with Cs deposited at 293 K show essentially the same C 1*s* spectrum as the pristine MWNTs, although Cs was also detected by photoemission spectroscopy. More recently, as reported by Bennich *et al.*,[22] a similar tail structure and energy shift were clearly observed in C 1*s* spectra of K deposited graphite even for low K coverage [0.1 monolayer (ML)]. Thus, the spectral broadening may originate in alkali-metal atoms on the nanotube (graphite) surface. Therefore, the temperature effect on the C 1*s* and Cs 4*d* spectra can be tentatively attributed to two different locations of the Cs atoms, one inside the MWNTs (between adjacent graphene sheets) and the other on the tube surfaces. Another possible explanation for the broadening is surface contamination that originates in Cs for the topmost surface of the nanotubes, because it is very likely that Cs on the topmost surface is easily degraded even in ultrahigh vacuum. At any rate, in the case of Cs deposition at 373 K, we cannot exclude the possibility that at least part of the Cs is not located inside the MWNTs, but on the tube surfaces. This suggests that some Cs deposited on the tips diffused onto the surface of the nanotubes. On the other hand, in the case of 293 K, the Cs atoms seem to be located inside the MWNTs due to the intercalation reaction, not on the tube surfaces.

Let us now compare the present results for the mobility of Cs with the in-plane Cs diffusion constant in graphite at room temperature, 2×10^{-5} cm^2/s.[23] This value is seven orders of magnitude larger than that found for the Cs diffusion constant of the MWNTs. Such a large difference is surprising because Cs atoms in MWNTs are located between adjacent graphene sheets, as well as in the Cs-intercalated graphite. As discussed in Ref. 24, the occurrence of the intercalation reaction in a MWNT indicates that a MWNT does not have an ideal (close-packed) structure. According to our previous studies, MWNTs, in general, contain a large number of defects.[7,25] This suggests that a possible reason for the extremely small diffusion constant is the hindrance of diffusion by the defects (breaks in the graphene sheets), which are specific in MWNTs. On the other hand, however, according to a recent study by electrochemical impedance spectroscopy, the Li diffusion constant in SWNT bundles at room temperature was estimated to also be very small, 1.5×10^{-12} cm^2/s,[26] whereas that in graphite even in the direction perpendicular to the basal plane was reported to be 2.1×10^{-10} cm^2/s.[27] If the Li diffusion constant in SWNTs is indeed that small, small diffusion constants might be specific to nanometer scale tubular structures regardless of the number of graphene sheet(s). Confirming this seems to require further investigation.

V. CONCLUSION

The Cs diffusion process in MWNTs was directly visualized using Cs 4*d* photoelectron microscopy. Cs, initially deposited on the tips of aligned MWNTs, diffused toward the roots by intercalation reaction at 293 K. The Cs diffusion constant in the MWNTs was evaluated to be 2×10^{-12} cm^2/s, which is seven orders smaller than that in graphite. At 373 K, Cs diffused more quickly, and the diffusion constant, which was possibly affected by surface diffusion, was evaluated to be larger than 8×10^{-11} cm^2/s.

The extremely small diffusion constant is quite surprising because Cs atoms are located between adjacent graphene sheets in intercalated MWNTs and graphite. Further investigation should answer the question whether such a small diffusion constant is a characteristic of defective MWNTs or of nanometer scale tubular structures.

ACKNOWLEDGMENTS

The authors thank Diego Lonza for excellent technical support in the SPEM experiments. Work done at NTT was partly supported by Special Coordination Funds of the Science and Technology Agency of the Japanese government and by a NEDO International Joint Research grant. Work done at the University of North Carolina was supported by the Office of Naval Research through a MURI program Grant (No. N0001-98-1-0597).

[1] R. S. Lee, H. J. Kim, J. E. Fischer, A. Thess, and R. E. Smalley, Nature (London) **388**, 255 (1997).
[2] A. M. Rao, P. C. Eklund, S. Bandow, A. Thess, and R. E. Smalley, Nature (London) **388**, 257 (1997).
[3] R. S. Lee, H. J. Kim, J. E. Fischer, J. Lefebvre, M. Radosavljevic, J. Hone, and A. T. Johnson, Phys. Rev. B **61**, 4526 (2000).
[4] A. Q. Wadlhawan, R. E. Stallcup II, and J. M. Perez, Appl. Phys. Lett. **78**, 108 (2001).
[5] H. Shimoda, B. Gao, X. P. Tang, A. Kleinhammes, L. Fleming, Y. Wu, and O. Zhou, Phys. Rev. Lett. **88**, 015502 (2002).
[6] E. Frackowiak, S. Gautier, H. Gaucher, S. Bonnamy, and F. Beguin, Carbon **37**, 61 (1999).
[7] S. Suzuki and M. Tomita, J. Appl. Phys. **79**, 3739 (1996).
[8] S. Suzuki, C. Bower, and O. Zhou, Chem. Phys. Lett. **285**, 230 (1998).
[9] C. Bower, S. Suzuki, K. Tanigaki, and O. Zhou, Appl. Phys. A: Mater. Sci. Process. **67**, 47 (1998).
[10] K. Hirahara, S. Bandow, K. Suenaga, H. Kato, T. Okazaki, H. Shinohara, and S. Iijima, Phys. Rev. B **64**, 115420 (2001).
[11] X. Fan, E. C. Dickey, P. C. Eklund, K. A. Williams, L. Grigorian, R. Buczko, S. T. Pantelides, and S. J. Pennycook, Phys. Rev. Lett. **84**, 4621 (2000).
[12] S. Suzuki *et al.*, Phys. Rev. B **66**, 035414 (2002).
[13] M. Marsi, L. Casalis, L. Gregoratti, S. Gunther, A. Kolmakov, J. Kovac, D. Lonza, and M. Kiskinova, J. Electron Spectrosc. Relat. Phenom. **84**, 73 (1997).
[14] M. Kiskinova, M. Marsi, E. DiFabrizio, and M. Gentili, Surf. Rev. Lett. **6**, 265 (1999).
[15] C. Bower, O. Zhou, W. Zhu, D. J. Werder, and S. Jin, Appl. Phys. Lett. **77**, 2767 (2000).
[16] C. Bower, W. Zhu, S. Jin, and O. Zhou, Appl. Phys. Lett. **77**, 830 (2000).
[17] S. Suzuki, Y. Watanabe, T. Kiyokura, K. G. Nath, T. Ogino, S. Heun, W. Zhou, C. Bower, and O. Zhou, Surf. Rev. Lett. **9**, 431 (2002).
[18] M. Kiskinova, Int. J. Imaging Syst. Technol. **8**, 462 (1997).
[19] S. Gunther, A. Kolmakov, J. Kovac, and M. Kiskinova, Ultramicroscopy **75**, 35 (1998).
[20] S. B. DiCenzo, S. Basu, G. K. Wertheim, D. N. E. Buchanan, and J. E. Fischer, Phys. Rev. B **25**, 620 (1982).
[21] R. Schlogl, in *Graphite Intercalation Compounds II*, edited by H. Zabel and S. A. Solin (Springer, Berlin, 1992), Chap. 3.
[22] P. Bennich, C. Puglia, P. A. Bruhwiler, A. Nilsson, A. J. Maxwell, A. Sandell, N. Martensson, and P. Rudolf, Phys. Rev. B **59**, 8292 (1999).
[23] H. Zabel, A. Magerl, J. J. Rush, and M. E. Misenheimer, Phys. Rev. B **40**, 7616 (1989).
[24] O. Zhou, R. M. Fleming, D. W. Murphy, C. H. Chen, R. C. Haddon, A. P. Ramirez, and S. H. Glarum, Science **263**, 1744 (1994).
[25] S. Suzuki, Y. Watanabe, T. Kiyokura, K. G. Nath, T. Ogino, S. Heun, W. Zhu, C. Bower, and O. Zhou, Phys. Rev. B **63**, 245418 (2001).
[26] A. Claye, J. E. Fischer, and A. Metrot, Chem. Phys. Lett. **330**, 61 (2000).
[27] N. Itoh, H. Toyoda, K. Morita, and H. Sugai, J. Nucl. Mater. **290–293**, 281 (2001).